Thermal structuring of metal-semiconductor core fibres: toward optoelectronic device fabrication

Seunghan Song
Norwegian University of Science and Technology
Fredrik Laurell
KTH Royal Institute of Technology
Bailey Meehan
Clemson University
Thomas Hawkins
Clemson University
John Ballato
Clemson University https://orcid.org/0000-0001-5910-3504
Ursula Gibson (ugibson@clemson.edu)
Clemson University https://orcid.org/0000-0002-8548-8791

Article

Keywords: glass-clad fibre, metal and semiconducting components, III-V GaSb, Group IV Si

Posted Date: November 18th, 2021

DOI: https://doi.org/10.21203/rs.3.rs-1009349/v1

Version of Record: A version of this preprint was published at Nature Communications on May 13th, 2022. See the published version at https://doi.org/10.1038/s41467-022-29975-1.

Thermal structuring of metal-semiconductor core fibres: toward optoelectronic device fabrication

Seunghan Song[1,+], Fredrik Laurell[2], Bailey Meehan[3], Thomas Hawkins[3], John Ballato[3], and Ursula Gibson[1,2,3,+,*]

[1]Norwegian University of Science and Technology, Physics Dept, Trondheim 7049 Norway
[2]KTH Applied Physics 10691 Stockholm Sweden
[3]Department of Materials Science and Engineering, Clemson University, Clemson, SC, 29634, USA
[*]ugibson@clemson.edu
[+]these authors contributed equally to this work

ABSTRACT

Combining metal and semiconducting components in the core of a glass-clad fibre brings new breadth to the range of structures that can be fabricated using localized thermal gradients. Both axial and lateral structuring of fibres drawn with multiple components is demonstrated, as well as the introduction, segregation and chemical reaction of metal components within an initially pure silicon core. Gold and tin longitudinal electrodes fabrication, segregation of GaSb and Si in an initially inhomogeneous fiber into parallel axial layers and Al doping of a GaSb core were demonstrated. Gold was introduced into Si fibers to purify the core or weld an exposed core to a Si wafer. Ga and Sb introduced from opposite ends of a silicon fibre reacted to form III-V GaSb within the Group IV Si host, as confirmed by structural and chemical analysis and room temperature photoluminescence.

Introduction

Interest in novel core fibres as a platform for electronic and optical applications is growing, as evidenced by a number of recent review articles.[1–4] Dramatic improvement in the optical transparency[5,6]of silicon core fibres has been made, and non-linear optical behavior is now well established.[7] One of the driving forces for the development of semiconductor cores has been the potential for optoelectronic devices, and prototype devices have been made in Group IV semiconductor core fibres,[8,9] using Si as well as SiGe. Detector development and solar conversion are of particular interest, but material quality, doping and electrode formation are challenging[8,10–12] for inorganic core materials due to the high processing temperatures involved. Post-processing of as-drawn fibre has been employed to improve the properties of the Group IV core materials, which are typically inhomogeneous and/or polycrystalline as drawn, with impurities at the grain boundaries.[13] To date the emphasis has been on using laser heating to recrystallize and homogenize the core,[14] and structuring of the core composition profile has recently been demonstrated in the silicon-germanium alloy system.[15–17]

Post-draw spatial segregation has also been demonstrated for (pseudo)eutectic Si-GaSb[18] and Au-Si.[6] During processing, laser induced thermal gradients create a higher concentration of the lower melting point material at the laser focus through the thermomigration process. This liquid alloy can then be translated through the core of the fibre in a miniature version of traveling solvent float zone (TSFZ) recrystallization or can be solidified in a controlled manner to structure the core. As the laser power is reduced, the lower melting point constituent segregates from the silicon, and the construction of two-component segregated structures within the core of a molten core drawn fibre has been demonstrated.[18] In this work, thermomigration is employed to rearrange the constituents of the fibre core, and combined with a traveling melt zone (which may or may not extend across the entire core) to recrystallize the material in a range of structures.

Thermomigration and Zone Melting

Thermomigration in semiconductors occurs when the composition and temperature of an alloy are non-uniform, with a solvent phase, typically a low melting point metal alloy, forming a droplet that will migrate towards the highest temperature point through the solid host material. The solubility of the majority constituent (Si, in most studies) is higher at the hot side of the melt, and the resulting concentration gradient drives diffusion across the droplet. Supersaturation at the cooler side of the melt leads to solidification, and this mass displacement translates the melt zone towards the high temperature. This process can be used to rearrange the components of a multimaterial fibre. Fig. 1 schematically presents several device-oriented experiments that were performed using laser-generated thermal gradients; **a-c**,introduction of one or more metallic elements into silicon

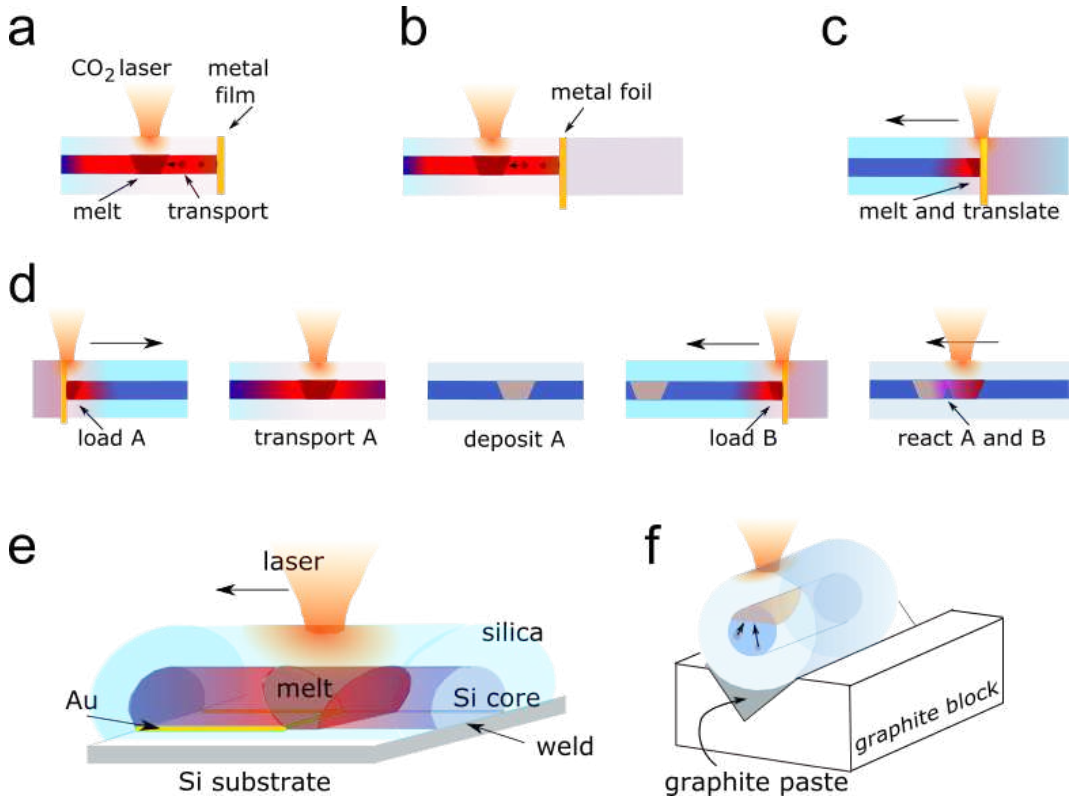

Figure 1. Schematic of sample preparation methods. a) Thermomigration of metal from a film deposited on the fibre end, driven by CO_2 laser heating, b)thermomigration from a metal foil pressed against the semiconductor core fibre, c)bulk dissolution of a foil into the semiconductor core, followed by translation, d) sequential introduction steps used to drive in-core formation of compounds, e) use of solvent (Au) layer and traveling melt zone to weld the silicon core of a fibre to a silicon substrate, and f) use of graphite as a thermal sink to establish a strong vertical component to the thermal gradient, driving thermomigration segregation of eutectic components within the fibre core.

core fibres, followed by translation of the melt zone within the fibre, **d** reactive formation of compounds within the silicon host, **e** welding of semiconductor core fibres to a substrate using a thin solvent layer to seed local melting and attachment of the fibre core, and **f** use of lateral thermal gradients to segregate immiscible components, thus either establishing either a conductive electrode along the side of the fibre core or a longitudinal structure with two semiconductors side by side.

In early studies, thermomigration was explored as a potential method for localized doping,[19,20] device formation,[21] recrystallization, and joining of silicon wafers.[22] Thermal gradients were typically less than 100 C cm^{-1}, and large cross-section samples led to poorly controlled trajectories.[23] A useful overview of the process is provided by Cline and Anthony[24] based on their doping of semiconductors, primarily Si. Studies of thermomigration continue, as the temperature gradients across microelectronic bump solders[25] can exceed 1000 K cm^{-1}, and associated segregation can lead to failure. The process is also employed for growth and modification of nanowires.[26–28]

In a simplified model, the migration rate, V, can be written as

$$V = \frac{(-D)}{(1-X_1)} \frac{\partial X_1}{\partial T} \nabla T$$

where X_1 is the concentration of Si in the liquid, $\partial X_1/\partial T$ is the local slope of the liquidus at composition X_1, ∇T is the temperature gradient across the liquid drop, and D is the diffusivity of Si in the liquid.[29] This model was used to derive droplet velocity predictions for several metals in Si.[24] Figure 2a shows calculated thermomigration velocities, normalized to the temperature gradient ∇T as function of inverse temperature for gold, gallium, and antimony[24] in Si, as well as experimental values for two gold droplets from the present work, discussed in more detail below. While not all considerations (e.g. chemical potential) are included, the model provides guidance for design and interpretation of experiments. The relative values of the velocities for different metals should be valid in large core fibres as well as bulk solids, so for example, gold should be more rapidly transported through silicon than antimony given the same thermal gradient. The parameters indicate the relative ease of

making structures using thermally driven transport in the fibre core. The thermomigration velocity measured for gold in the previous work, with a temperature gradient of 50 K cm^{-1}, was 0.05 μm s^{-1}, at a temperature of 930 °C. As the temperature and temperature gradient increase, improved solubility and transport of silicon across the gold alloy liquid region lead to more rapid translation of the liquid drop through the solid, with laser heated droplet velocities as high as 100 μm s^{-1}.

The temperature gradient in the laser treated material in this work is 100 times greater than in the bulk studies at comparable temperatures,[24] yet the agreement between the model and these experiments is excellent, emphasizing the importance of near-equilibrium thermodynamics in the process.

If sufficient solvent is accumulated in a confined geometry such as a fibre core, the melt will span the diameter of the core and the melt zone position and velocity can be controlled by the (laser) heat source. When the hot zone is translated slowly, the result is similar to traveling melt zone refinement. The traveling melt zone processing has been used in ingot refining (as the solubility of impurities is higher in the melt than the solid) since the 1950s,[30] for both elemental and compound samples, and a more recent review[31] emphasizes its wide applicability. In semiconductor fibres, where unary fibres typically are drawn with polycrystalline cores, an alloying element can suppress nucleation,[15] promoting the growth of long single crystals, even when compositional inhomogeneity is significant. During laser heating of these materials, thermomigration of liquid droplets can be observed,[15] and the accumulation of solvent to form a core-spanning melt zone can esteblish a traveling solvent floating zone (TSFZ) process, with the translation rate of the heat source chosen to optimize the formation of large grains. The choice of thermal gradient and annealing speed for fibre crystallization, as noted by Badding[32] is critical, and fundamental studies of thermomigration may provide important modeling information. With a melt zone traveling through an alloy, the scanning velocity relative to the thermomigration velocity will determine whether the droplets (and hence a compositionally enriched region) can match the speed of the heater, or if some material will lag, leaving a trail of solidified solvent. The finite thermomogration velocity helps clarify the inhomogeneity of SiGe as-drawn material;[15] the thermal gradient of the drawing tower is small compared to that induced by the laser, and drawing speeds are on the order of m min^{-1}. SiGe forms a solid solution, so gradient composition structures are formed,[15] but for a eutectic system, any solvent residue will phase segregate upon solidification, with the cooling geometry and heat source velocity determining the location of the segregated components.

In this work, a CO_2 laser is employed to establish thermal gradients with different radial and azimuthal profiles, and thermomigration and TSFZ processes were used to fabricate novel in-core structures in semiconductor core fibres.

Results and discussion

As a fundamental study to assure that, at the large thermal gradients induced during laser treatment of silicon fibres, thermomigration is still adequately described by simple models, the velocity of Au droplets moving through Si core fibres was measured. In addition, the use of this process for recrystallization and reconfiguration of the components of composite metal-semiconductor core fibres was explored.

Metal introduction and removal from silicon

The use of an alloying element such as Ge in Si core fibre lowers the melting temperature off the core significantly and suppress nucleation during solidification,[15] promoting the formation of longer single grain regions in the highly crystalline cores. For materials with a low solid solubility in Si that form a eutectics (or pseudo-eutectics) rather than a solid solution, the added element (compound) can be removed during the recrystallization process. This concept was demonstrated with a small amount of gold that was introduced to silicon core fibres, translated to recrystallize and purify the material, then removed. In addition, the use of a metal for welding of an exposed fibre core to a Si substrate (with subsequent removal of the solvent phase) was demonstrated. Supplementary Information Fig.1 and 2 document doping of the core by thermal gradient introduction of metal elements to a semiconductor core fibre.

Au thermomigration in Si core fibre

For fundamental studies of thermomigration, one end of a silicon core fibre, fabricated using the molten core method on a draw tower,[15] was coated with 500nm of vapor-deposited Au. A slow increase of the laser power at a distance of $\sim$ 500 μm from the end of the fibre allowed microscopic observation of the dynamics of the thermomigration of small droplets of liquid through the core. Velocity measurements were extracted from the positional information in video frames acquired during the heating. As the silicon core is of high purity both before and after the transition of an alloy droplet, modeling the temperature and temperature gradient using the blackbody emission is a good approximation,[14] with the edge of the laser-induced melt zone of the pure core (ahead of the droplet) providing a temperature calibration point. The temperature gradient was found to be 4500-5500K cm^{-1}, and was approximately uniform over the observable travel range of more than 500 μm. Velocity data normalized by the temperature gradient, from the trajectories of two particles, is shown in Fig.2a as a function of temperature, demonstrating a high degree of repeatability. Also plotted are literature values of the gradient-normalized velocity at 50K cm^{-1}, with the theory from Anthony and Cline.[29,33] Their straightforward model predicts the observed increase in slope at high

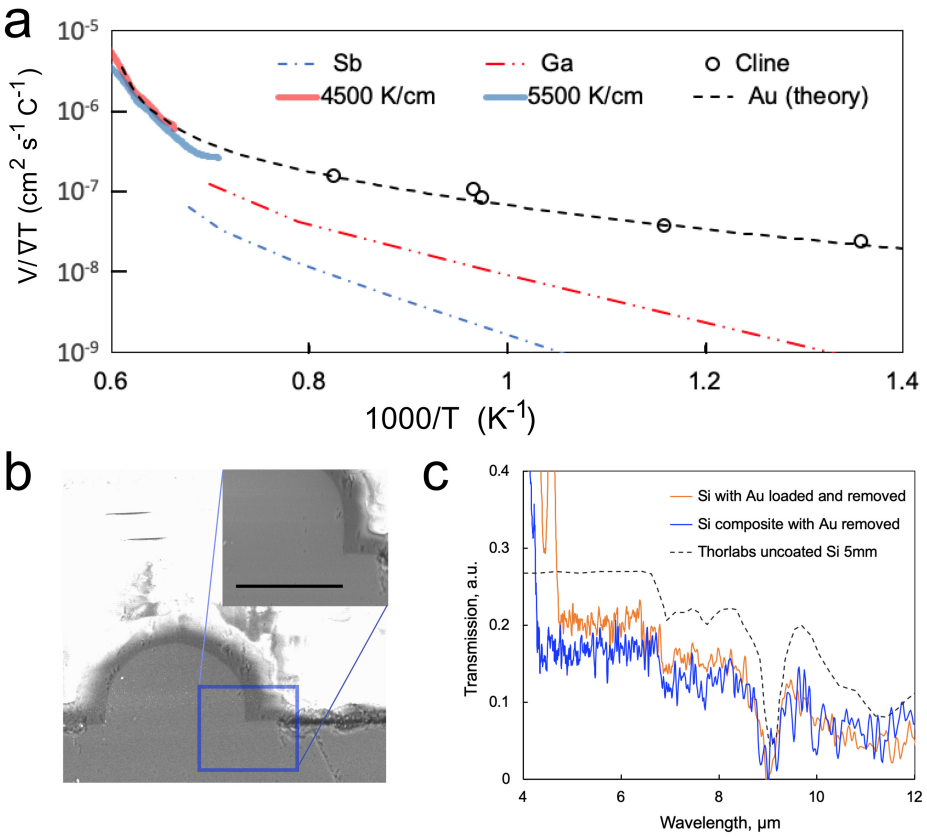

Figure 2. Thermomigration of Au in Si. a) Calculated and experimental alloy droplet velocity in silicon normalized by the temperature gradient in the host, as a function of 1/T for several metals; theory and data for Au in Si after Cline and Anthony,[24,33] with experimental data from two droplets in the present study (solid lines- orange for the gradient of 4500K cm^{-1} and blue for the gradient of 5500K cm^{-1}). b) Si fibre core welded to a single crystal Si substrate after thermomigration removal of a thin Au layer at the interface (inset close-up of weld region, scale bar 50 μm), and c) Infrared transmission of Si fibres after removal of gold that was introduced by thermomigration (orange) and by inclusion in the preform when drawing the fibre(blue). The black dashed curve shows the transmission profile of a 5mm thick uncoated Si window (Thorlabs), normalized to allow comparison of spectral features.

temperatures, with good agreement between experiment and theory even at the high temperatures and gradients imposed here. The laser heating results demonstrate the robust nature of Au alloy thermomigration, and the utility of simple models to predict the conditions necessary for processing.

Substrate welding

Thermomigration with a solvent metal can be also used to form a bond between exposed fibre core and a substrate, a method related to earlier wafer packaging work by Rudakov.[22] The cladding glass was removed from one side of a piece of silicon core fibre containing 5% Sn (to reduce the temperature required for recrystallization). This fibre was placed onto a silicon substrate coated with gold. With CO_2 laser heating, the gold and Sn melted and were drawn away from the interface, leaving the Si fibre core welded to the substrate surface with no detectable interfacial discontinuity, as shown in Fig 2b. The use of a solvent layer may enable laser writing of out-of-plane waveguides,[34,35] using single crystal substrates as a crystalline template.

Solvent refining

Previous results on the gold-silicon system demonstrated enhanced infrared transparency of a silicon core fibre after a laser-based gold extraction treatment,[6] resulting from recrystallization of the Si. In that study, gold was removed from silicon (90 at. %)-gold (10 at.%) composite fibres, demonstrating the utility of gold as a solvent for refinement of silicon core optical fibres. However, when the gold is a constituent of the drawn fibre, refined sample length is limited by the accumulation of gold at the laser focus; eventually the melt zone size exceeded the laser beam diameter and excess gold is deposited in the recrystallized Si. To overcome this limitation for the fabrication of long samples, a small bolus of gold was introduced into the core of a pure

silicon fibre. This allowed translation of the gold-rich melt zone along the host fibre for macroscopic distances, with a high degree of control over the translation speed of the solidification front.

Figure 2c provides FTIR transmission results for a silicon core fibre recrystallized after thermomigration loading of a small amount of gold and subsequent translation of the laser-induced alloy melt zone a distance of 2.2 cm along the fibre. Also shown is data for a 1cm composite Au-Si fibre from which gold was removed. The transparency of the thermomigration-refined sample suggests that this is a scaleable method for production of far infrared transparent fibre. Supplementary Information Fig. 3 presents XRD results for the as-drawn and gold-bolus refined samples, showing the latter is composed of only two grains.

Lateral segregation

In eutectic multiphase fibres, whether as-drawn composites or pure fibres with a metal introduced by thermomigration, the gradients applied during subsequent processing determine the geometric distribution of the phases upon solidification. A strong lateral (perpendicular to the axis) gradient can be established if the fibre is thermally coupled to a substrate during laser treatment. With suitable translation speed of the heat source, thermomigration towards the laser and subsequent solidification can result in the formation of laterally segregated materials over cm distances. This segregation has been performed with as-drawn eutectic Si-Au, Si:Sn and Si-GaSb, as well as fibres where the metal was thermally drawn into a pure silicon fibre, then segregated to one side locally as seen in Fig 3.

Au and Sn electrodes

Figure 3a,b, shows XCT results for a fibre drawn with a 10 at% Au in Si core, with Fig 3c the result of laser treatment that formed a continuous filament of gold on the heated side. The transport of gold across the core is primarily by a thermomigration mechanism, and the temperature gradient sufficient to cause transport across the fibre must be balanced by a laser translation rate that prevents the melt zone from spanning the entire core. It is worth noting that the thermal properties of the cladding-substrate system play a role in the ability to establish this balance, with heat capacity, coupling and cooling efficiency of the materials all of importance. For 3d-g, a small amount of tin was thermally drawn into a pure silicon fibre, and the laser beam was translated at a sufficiently high speed to restrict the melt zone to the laser-side of the fibre. In this case, a Sn-rich electrode was deposited over a finite distance, limited by the supply of Sn that was introduced through the end of the fibre.

Si-GaSb

The lateral segregation method can also be used for fibres drawn with mixed semiconductors having a pseudo-eutectic phase diagram, such as Si:GaSb.[18] In Fig 3 h,i, the formation of two distinct layers is demonstrated using this system. The power and scan rates were adjusted to allow thermomigration of the GaSb to the heated side of the fibre, and graphite was used to maintain the other side of the fibre below the melting point of pure silicon. A thread of GaSb extruded into a stress-induced crack in the silicon core during solidification. Preliminary investigation of the production of Bragg gratings in this system are presented in Supplementary Information Fig.4.

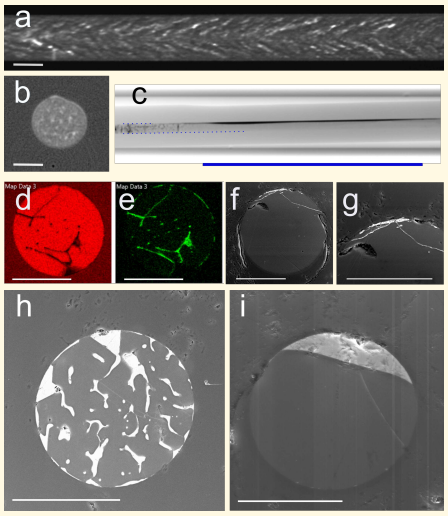

Figure 3. Lateral segregation of fibre components (a-c) Si-Au, (d-g) Si-Sn and (h, i) Si-GaSb **a** side XCT of as-drawn Si-Au **b** Cross sectional XCT of as-drawn Si-Au **c** Side XCT of Si-Au after lateral segregation. Thin dotted blue lines highlight the edges of the Si core to the left of the treated area. **d** EDS of Si in Si-Sn as drawn fibre, **e** EDS of Sn, **f** BSE of Si-Sn core after segregation, and **g** closeup of Sn region showing extrusion into stress crack in Sn. **h** BSE image of as-drawn Si-GaSb core fibre, and **i** Si-GaSb after segregation. Scale bars 100μm except in **b**, 4mm

Reactive formation of compounds

Using endface or side-groove introduction, multiple elements can either be brought in sequentially from one side, or introduced from opposite directions. This technique was used to synthesize inclusions of III-V compounds inside a silicon core. The introduction and translation of the constituent elements, which have eutectic temperatures in Si well below the melting point of the target compound, allows localization of the reaction product.

Metal introduction and reaction: GaSb fabrication in Si

Formation of a localized deposit of III-V material within a silicon core was demonstrated by first thermally drawing Sb through one endface of a 2cm long fibre, and subsequently drawing Ga into the other end. Each of the solvent metals was transported to the midpoint of the fibre using the laser to draw a full-width melt zone along the fibre to the reaction zone. A scanning electron microscope (SEM) image of the side polished fibre, along with Energy dispersive (EDS) X-ray results and photoluminescence spectrum are presented in Fig 4 a, b. While the rapid cooling of the sample due to the pre-programmed laser power steps

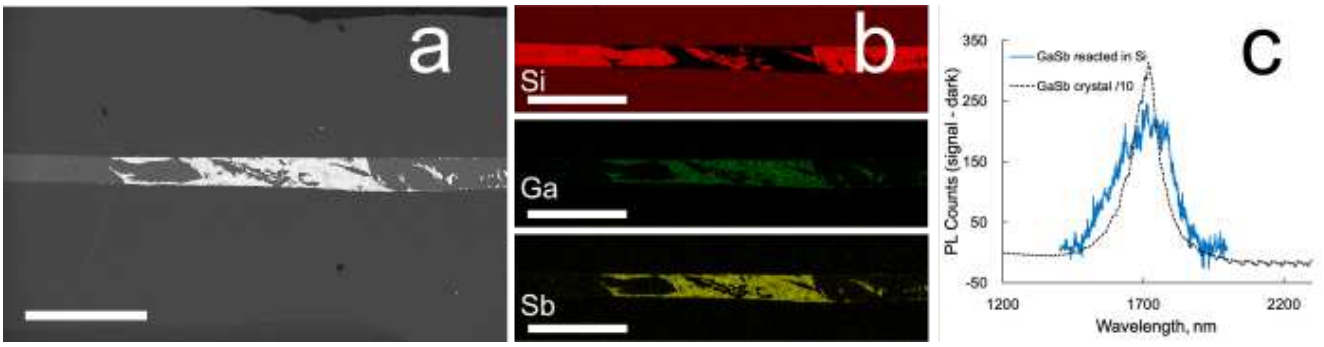

Figure 4. Results on GaSb reactively formed inside the Si core of a fibre at the midpoint of a 2 cm sample a) Backscattered SEM image of GaSb (bright areas) inside a silicon fibre core. Ga was thermally directed from the left and Sb was brought in from the right. b) EDS results showing Si (top), Ga(middle), and Sb (bottom panel), demonstrating good segregation of GaSb from Si. Scale bars 500μm. c)GaSb photoluminescence measurements excited with 532 nm radiation for single crystal bulk material (dashed black curve; values divided by 10), and GaSb synthesized within the silicon fibre (blue curve).

resulted in some commingling of the silicon and GaSb regions, the localized deposit suggests that a more gentle cooling, accompanied by a slow translation, would result in silicon deposition at one region of the solidification zone, followed by a block of GaSb. If an excess of one solvent metal is present, translation at lower power during cooling could be used to promote recrystallization of the GaSb, in analogy with the Au crystallization of Si. Residual metal could then be transported out through the side of the silicon through which it was introduced. In some samples, residual Sb (but not Ga) was observed by XCT (Supplementary Information Fig 5) in the loading side of the fiber, likely associated with the slower diffusion of this material in Si (See Fig.3).

EDS results clearly demonstrate the presence of a mixture of GaSb and Si over a distance of 1 mm, and room temperature photoluminescence was observed from the reactively formed material, as shown in Fig.4c. These results were obtained from the fibre that was polished for the SEM studies, to assure analysis of the same regions. Raman data (Supplementary Information Fig.6) taken before polishing the fiber, confirm GaSb formation, and the lone transverse optical (TO) peak suggests a high degree of crystalline order.

One of the possibilities raised by the assembly of the components from opposite ends of the fibre is that of creating a light emitting diode - with p-dopants and n-type dopants in the ends of the silicon with a compound light emitting material in the center. A two point measurement of the fiber resistance gave R=$10^5\Omega$, suggesting high doping levels. Production of this type of device will require more sophisticated control of the amounts of metal delivered to the reaction zone.

Methods

The studies reported here were performed on silicon core, silica clad fibres with outer diameters from 0.5 mm to 1.5 mm and a core radius one tenth of the silica diameter. Fibers were made using the molten core draw method, with 3 cm silica preforms, and a temperature of $\sim$ 1950 °C. Pure silicon (ρ >4800 Ω cm) core fibre was used for the metal introduction and recrystallization studies, while 10% Au[6] and 30% GaSb in silicon[18] cores were used for lateral segregation of composites. Sn was introduced into a pure silicon core to demonstrate the feasibility of lateral segregation following metal introduction. Ga metal (99.995) and >99% purity Sn, Sb and Al foils from Alfa Aesar were used as metal sources.

Analysis

A Bruker DaVinci powder diffractometer with a 15 mm diameter beam from a Mo Kα1,2 X-ray source (λ=0.07093nm, 0.071359 nm) was used in this work. The silica is sufficiently transparent at these wavelengths to permit analysis of the crystalline core without removal of the cladding. Samples were rotated at 1 Hz during Bragg scattering measurements, then strong reflections were analyzed as a function of the fibre rotational position. XCT was performed using a Bruker Skyscan 1172unit, at an acceleration voltage of 167 kV, source current of 59 μA, and image pixel size of 0.65 μm. FTIR data was

obtained with a Bruker Tensor 27, using a PIKE Technologies beam condenser. Images and movies of thermomigration were made using a Thorlabs DCU224C CCD camera, and position vs. time information was extracted using Python software Trackpy.[36]

0.1 Sample preparation

Metal introduction

The metal of interest was either vacuum deposited (Au) or melted (Ga, Sn) onto the end of the silicon core fibre, or a thin foil (Au, Au+Sb, Sn, Sb, Al) was clamped between the fibre and a silica rod of similar diameter. The core of the fibre was then laser heated sufficiently to form a melt zone at a distance of 0.2 mm from the end of the fibre. For some metals (Ga, Au), thermomigration was efficient, with droplets of liquid traveling through the solid near the end of the fibre and a gradual increase in the size of the melt zone. For other elements, an oxide layer hindered metal uptake, and it was preferable to extend the melt zone to the end of the core, forming direct contact between the molten Si and the desired inclusion. Typical CO_2 laser power levels were between 9 and 15W, and scan rates were 10-20 μm s^{-1}.

Traveling melt zone recrystallization

Translation of the alloy melt zone was performed by relative motion of the fibre and laser, with typical velocities of 10-25 μm s^{-1}, while maintaining a melt zone width of 0.5 to 2mm. Slow reduction of power was used to suppress stress cracking as the core material solidified. Although the metal component would be expected to shrink and ameliorate the expansion of the silicon on cooling, in eutectic systems, the attractive interaction in the liquid phase leads to expansion of several percent upon solidificatio.[37]

Lateral segregation

For radially symmetric laser treatment of novel core fibres, the laser creates a melt zone that is uniform or nearly so across the diameter of the core. Even with unilateral heating, typical phase boundaries have an angle of greater than 75° with respect to the axis. To segregate the components laterally, one side of the fibre is thermally coupled to a graphite block while the laser is incident on the other. In this work, a 1 cm square cross section graphite block was used to support the silica-clad fibre. To assure uniform thermal contact, a v-groove of depth 0.5 mm was machined along the block. This groove was loaded with a small amount of Aquadag® graphite liquid suspension into which the fibre was placed. The power level, spot size and translation rate were adjusted to allow thermomigration from the cold side of the fibre, without accumulating so much of the alloying element that the melt zone extended across the full diameter. Laser spot sizes up to 1mm were used in combination with translation rates up to 50 μm cm^{-1} for fibres of 0.5-1.3 mm outer diameter.

1 Data Availability

Data is available upon request from the corresponding author.

References

1. Loke, G., Yan, W., Khudiyev, T., Noel, G. & Fink, Y. Recent progress and perspectives of thermally drawn multimaterial fiber electronics. *Adv. Mater.* **32**, 1904911, DOI: https://doi.org/10.1002/adma.201904911 (2020). https://onlinelibrary.wiley.com/doi/pdf/10.1002/adma.201904911.
2. Peacock, A. C. In-fiber semiconductor photonics: a new platform for nonlinear applications. vol. 11770 of *Proc.SPIE Proceedings Volume 11770, Nonlinear Optics and Applications XII; 1177002*, DOI: 10.1117/12.2596857 (2021).
3. Gibson, U. J., Wei, L. & Ballato, J. Semiconductor core fibres: materials science in a bottle. *Nat. Commun.* **12**, 3990, DOI: 10.1038/s41467-021-24135-3 (2021).
4. Stefani, A. *et al.* Multimaterial and flexible devices made by fiber drawing. In *2020 22nd International Conference on Transparent Optical Networks (ICTON)*, 1–3, DOI: 10.1109/ICTON51198.2020.9203327 (2020).
5. Ren, H. *et al.* Low-loss silicon core fibre platform for mid-infrared nonlinear photonics. *Light. Sci. & Appl.* **8**, 105, DOI: 10.1038/s41377-019-0217-z (2019).
6. Sørgård, T. *et al.* Broadband infrared and THz transmitting silicon core optical fiber. *Opt. Mater. Express* **10**, 2491–2499, DOI: 10.1364/OME.403591 (2020).
7. Peacock, A. C. *et al.* Wavelength conversion and supercontinuum generation in silicon optical fibers. *IEEE J. Sel. Top. Quantum Electron.* **24**, 1–9, DOI: 10.1109/JSTQE.2017.2762958 (2018).
8. Homa, D., Cito, A., Pickrell, G., Hill, C. & Scott, B. Silicon fiber with p-n junction. *Appl. Phys. Lett.* **105**, 122110, DOI: 10.1063/1.4895661 (2014). https://doi.org/10.1063/1.4895661.

9. Lei, W. *Optoelectronic Fibers*, 1335–1350 (Springer Singapore, Singapore, 2019).

10. Luo, Q. *et al.* Single crystal tellurium semiconductor core optical fibers. *Opt. Mater. Express* **10**, 1072–1082, DOI: 10.1364/OME.388187 (2020).

11. Huang, Y. P. & Wang, L. A. In-line silicon Schottky photodetectors on silicon cored fibers working in 1550 nm wavelength regimes. *Appl. Phys. Lett.* **106**, 191106, DOI: 10.1063/1.4919449 (2015). https://doi.org/10.1063/1.4919449.

12. He, R. *et al.* Silicon p-i-n junction fibers. *Adv. Mater.* **25**, 1461–1467, DOI: https://doi.org/10.1002/adma.201203879 (2013). https://onlinelibrary.wiley.com/doi/pdf/10.1002/adma.201203879.

13. Wei, W. *et al.* Single crystal semiconductor-core optical fiber. In Ballato, J. & Dong, L. (eds.) *Sixth Intl WSOF 2019*, vol. 11206;, 1120615:1–4, DOI: 10.1117/12.2557110 (SPIE, 2019).

14. Healy, N. *et al.* Co2 laser-induced directional recrystallization to produce single crystal silicon-core optical fibers with low loss. *Adv. Opt. Mater.* **4**, 1004–1008, DOI: https://doi.org/10.1002/adom.201500784 (2016). https://onlinelibrary.wiley.com/doi/pdf/10.1002/adom.201500784.

15. Coucheron, D. A. *et al.* Laser recrystallization and inscription of compositional microstructures in crystalline sige-core fibres. *Nat. Commun.* **7**, 13265, DOI: 10.1038/ncomms13265 (2016).

16. Wu, W. *et al.* Ge-capped sige core optical fibers. *Opt. Mater. Express* **9**, 4301–4306, DOI: 10.1364/OME.9.004301 (2019).

17. Wu, W. *et al.* CO_2 laser annealed SiGe core optical fibers with radial Ge concentration gradients. *Opt. Mater. Express* **10**, 926–936, DOI: 10.1364/OME.390482 (2020).

18. Song, S. *et al.* Laser restructuring and photoluminescence of glass-clad GaSb/Si-core optical fibres. *Nat. Commun.* **10**, 1790, DOI: 10.1038/s41467-019-09835-1 (2019).

19. Lomov, A., Seredin, B., Martyushov, S. Y., Zaichenko, A. & Shul'pina, I. The formation and structure of thermomigration silicon channels doped with ga. *Tech. Phys.* **66**, 453–460 (2021).

20. Cline, H. & Anthony, T. Thermomigration of aluminum-rich liquid wires through silicon. *J. Appl. Phys.* **47**, 2332–2336 (1976).

21. Kluge-Weiss, P. & Roggwiller, P. Laser-induced liquid zone migration of metal-silicon alloys in si. *MRS Online Proc. Libr.* **4**, 449–455, DOI: 10.1557/PROC-4-449 (1981).

22. Rudakov, V. & Plis, N. Aluminum thermomigration technology for fabrication of silicon packages. In *EuroSimE 2005. Proceedings of the 6th International Conference on Thermal, Mechanial and Multi-Physics Simulation and Experiments in Micro-Electronics and Micro-Systems, 2005.*, 325–329, DOI: 10.1109/ESIME.2005.1502822 (2005).

23. Mizrah, T. Joining and recrystallization of Si using the thermomigration process. *J. Appl. Phys.* **51**, 1207–1210, DOI: 10.1063/1.327689 (1980). https://doi.org/10.1063/1.327689.

24. Cline, H. E. & Anthony, T. R. Thermomigration of molten Ga in Si and GaAs. *J. Appl. Phys.* **48**, 2196–2201, DOI: 10.1063/1.324021 (1977). https://doi.org/10.1063/1.324021.

25. Shen, Y.-A., Zhou, S., Li, J., Tu, K. & Nishikawa, H. Thermomigration induced microstructure and property changes in sn-58bi solders. *Mater. Des.* **166**, 107619, DOI: https://doi.org/10.1016/j.matdes.2019.107619 (2019).

26. Xie, D.-G. *et al.* Controlled growth of single-crystalline metal nanowires via thermomigration across a nanoscale junction. *Nat. Commun.* **10**, 4478, DOI: 10.1038/s41467-019-12416-x (2019).

27. Bennett, P., Chobanian, J., Flege, J., Sutter, E. & Sutter, P. Surface thermomigration of nanoscale pt-si droplets on stepped si (100). *Phys. review. B, Condens. matter* **37**, DOI: 10.1103/PhysRevB.76.125410 (2007).

28. Eslamian, M. & Saghir, Z. Thermodiffusion applications in mems, nems and solar cell fabrication by thermal metal doping of semiconductors. *Fluid Dyn. Mater. Process.* **8**, 353–380 (2012).

29. Anthony, T. R. & Cline, H. E. Thermal migration of liquid droplets through solids. *J. Appl. Phys.* **42**, 3380–3387, DOI: 10.1063/1.1660741 (1971). https://doi.org/10.1063/1.1660741.

30. Pfann, W. G. Principles of zone-melting. *JOM* **4**, 747–753, DOI: 10.1007/BF03398137 (1952).

31. Koohpayeh, S. Single crystal growth by the traveling solvent technique: A review. *Prog. Cryst. Growth Charact. Mater.* **62**, 22–34, DOI: https://doi.org/10.1016/j.pcrysgrow.2016.03.001 (2016). Special Issue: Recent Progress on Fundamentals and Applications of Crystal Growth; Proceedings of the 16th International Summer School on Crystal Growth (ISSCG-16).

32. Ji, X. *et al.* Single-crystal silicon optical fiber by direct laser crystallization. *ACS Photonics* **4**, 85–92, DOI: 10.1021/acsphotonics.6b00584 (2017). https://doi.org/10.1021/acsphotonics.6b00584.

33. Anthony, T. R. & Cline, H. E. Thermomigration of Gold-Rich Droplets in Silicon. *J. Appl. Phys.* **43**, 2473–2476, DOI: 10.1063/1.1661534 (1972).

34. Aktas, O., Yamamoto, Y., Kaynak, M. & Peacock, A. C. Direct laser writing of graded-index SiGe waveguides via phase segregation. In Molpeceres, C., Qiao, J. & Narazaki, A. (eds.) *Laser Applications in Microelectronic and Optoelectronic Manufacturing (LAMOM) XXVI*, vol. 11673, 131 – 136. International Society for Optics and Photonics (SPIE, 2021).

35. Aktas, O. *et al.* Nonlinear properties of laser-processed polycrystalline silicon waveguides for integrated photonics. *Opt. Express* **28**, 29192–29201, DOI: 10.1364/OE.400536 (2020).

36. Allan, D. B., Caswell, T., Keim, N. C. & van der Wel, C. M. trackpy: Trackpy v0. 4.1. *Zenodo. CERN, Geneva, Switz.* (2018).

37. Rivlin, V. G., Waghorne, R. M. & Williams, G. I. The structure of gold alloys in the liquid state. *Gold Bull.* **9**, 84–87, DOI: 10.1007/BF03215410 (1976).

Acknowledgements

Funding sources –This work was supported by Norwegian Research Council grants 219686, 262644 and 262232, the Norwegian Micro-and Nano-Fabrication facility, NorFab, project number 245963/F50, Swedish Research Council (grant 2016–04488), the Swedish Foundation for Strategic Research (SSF) grant RMA15–0135, and the Knut and Alice Wallenberg Foundation grant 2016.0104 (UJG), the J. E Sirrine Foundation (JB).

Author contributions statement

U.J.G. conceived the experiments and performed the laser processing, S.S. provided the materials analysis and modeling. B.M., T.H., U.J.G. and J.B. produced the fibres. F.L. provided applications insight. All authors reviewed the manuscript.

Competing interests

The authors declare no competing interests.

Supplementary Files

This is a list of supplementary files associated with this preprint. Click to download.

- oct22supplementarymaterial.docx